SiD ECal Geometry

Amanda Steinhebel, James Brau
University of Oregon, Center for High Energy Physics,
1274 University of Oregon Eugene, Oregon 97403-1274 USA
(Dated: March 9, 2018)

I. ECAL OVERVIEW

In the validated SiD design, the electromagnetic calorimeter (ECal) barrel sits between the silicon tracker and the hadron calorimeter (HCal), at an inner radius of 1264 mm from the interaction point with a z extent of 3.53 m. It is made of twelve trapezoidal modules that extend the full z length of the detector. These modules have a small inner angle of 30^o and overlapping ends to avoid projective cracks through the detector. This creates a structure that is periodic in increments of $\pi/6$ radians. Figure 1 shows the view from the xy plane with the z dimension coming out of the page. The angle φ is also indicated.

Each module consists of 31 layers of tiled silicon wafers and 30 layers of DENS-24 tungsten alloy. The first layer of each module is a silicon tracking layer, followed by twenty iterations of 2.5 mm DENS-24 and a 1.25 mm gap in which the 0.3 mm silicon sensor layer resides, along with the KPiX ASIC readout chip (Fig. 2). This is followed by ten iterations of 5 mm DENS-24 and the same 1.25 mm silicon-containing gap. Therefore, the ECal begins and ends with a sensitive silicon layer. This structure is identically repeated for all twelve modules (Fig. 1).

The region of overlap between two modules, shown in the cutout of Fig. 1, spans from $\varphi \in [(4.03+30n)^o, (15+30n)^o]$, where n is an integer, $n = 0, 1, \ldots, 11$. This is approximately 30% of the detector. Showers that develop in this region deposit charge into both modules. Within $\varphi \in [(8.79 + 30n)^o, (10.14 + 30n)^o]$, showers would encounter only thin layers of tungsten absorber and no thicker 5 mm tungsten layers. This "thin overlap region" is due to the unequal distribution of tungsten absorber throughout each module.

All the following studies were conducted using the full SiD simulation, `SiD_o2_v02`. Five hundred single photons were directed into the full detector simulation, including a 5 T magnetic field, incident to the ECal surface ($\theta = 90^o$) with initial energies of 10 GeV and 100 GeV. Various φ angles were investigated ($\varphi = 0^o$, 3.25^o, 7.5^o, 9.3^o, 11.25^o, 15^o, 18.25^o, 26.25^o, and 30^o) in order to survey through one 30^o period of the detector. Within this set, two points fall in the overlap region ($\varphi = 7.5^o$ and 11.25^o) and one in the thin overlap region ($\varphi = 9.3^o$). Only charge deposited in the silicon layers of the ECal barrel was considered.

The tracking layer of silicon at the beginning of each module is excluded from these studies. In overlap regions, this layer falls near the middle of the calorimeter and samples showers before they have traversed a full absorber layer. In this sense, this portion of the shower is being double-sampled due to the presence of this sensitive layer. This conclusion has led the SiD collaboration to consider designing the modules so that the tracking silicon layer is only present around the inner circumference of the ECal. Reducing the extent of this layer can be a cost-saving method.

All figures shown here and raw data files can be found at `http://pages.uoregon.edu/asteinhe/SiDNotes/geometry/`, and the analysis scripts that generate them can be found at `https://github.com/SiliconDetector/UserAnalyses/tree/master/asteinhebel_ECalAnalysis/Geometry/`.

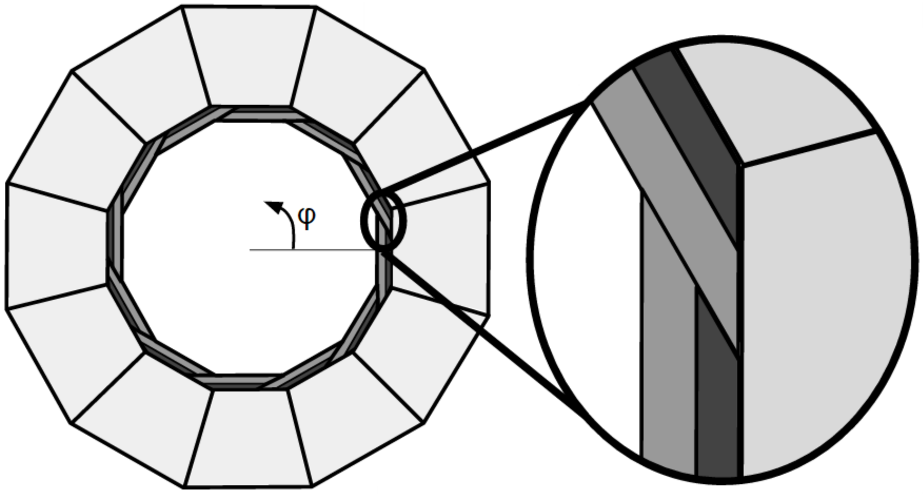

FIG. 1: The SiD ECal (darker shades) is surrounded by the hadron calorimeter (lightest shade) and made of twelve overlapping trapezoidal modules to avoid projective cracks. The cutout image illustrates the overlap region of these ECal modules, where the darkest shade indicates areas with thick tungsten layers and the medium-colored shade indicates areas with thin tungsten layers. The image shows the view from the xy plane with the z dimension coming out of the page, as well as the angle φ.

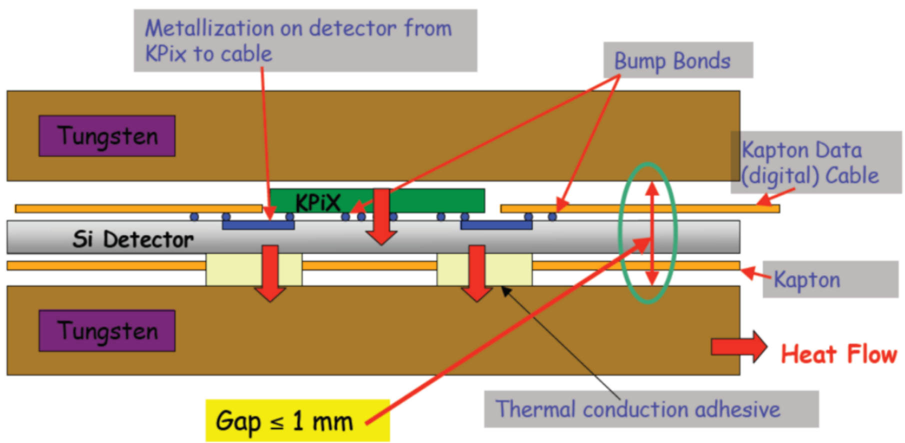

FIG. 2: The 1.25 mm gap between tungsten absorber layers includes a 0.3 mm silicon sensor layer bump-bonded to the KPiX readout chip. [Figure credit: Martin Breidenbach, SLAC]

II. FIGURES

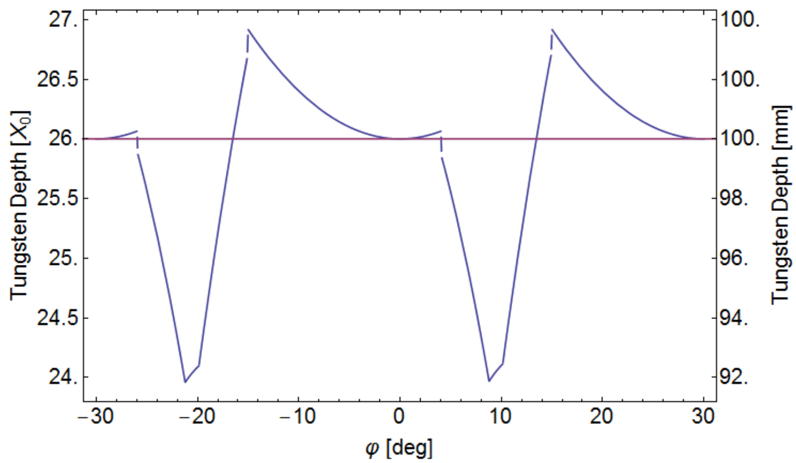

FIG. 3: Total thickness of DENS-24 in radiation lengths [X_0] in the ECal barrel at different φ positions. At normal incidence, there are 26 radiation lengths, but this decreases as φ increases and enters the overlap region ($\varphi = -25.97, 4.03$). At the beginning of the thin overlap region ($\varphi = -21.21, 8.79$), the module depth reaches a minimum of 23.7 X_0 before gaining depth again until encountering normal incidence in the next module. This variation means that electromagnetic showers develop differently within the calorimeter depending on the φ angle of incidence.

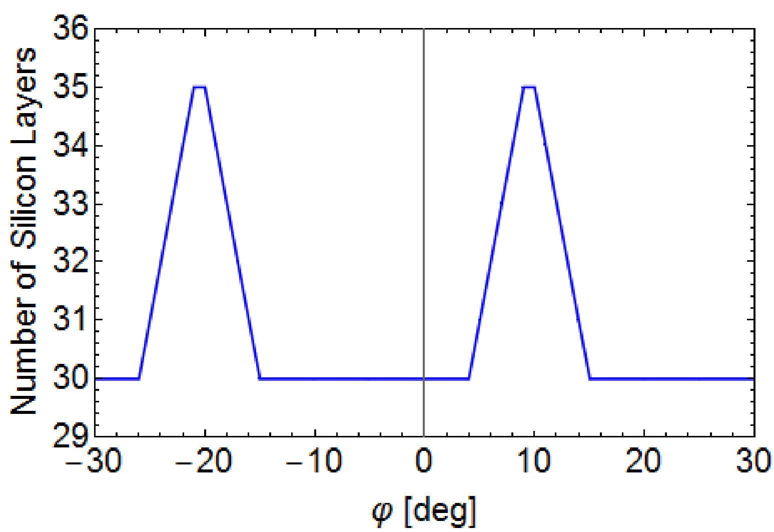

FIG. 4: Total number of silicon layers in the ECal barrel a shower would encounter at different φ positions, excluding the initial silicon tracking layer. At normal incidence, there are 30 silicon layers. At maximum, within the thin overlap region, there are 35 silicon layers. This, combined with a decrease in absorber thickness, creates a region that samples the shower differently (more often) than the region at normal incidence.

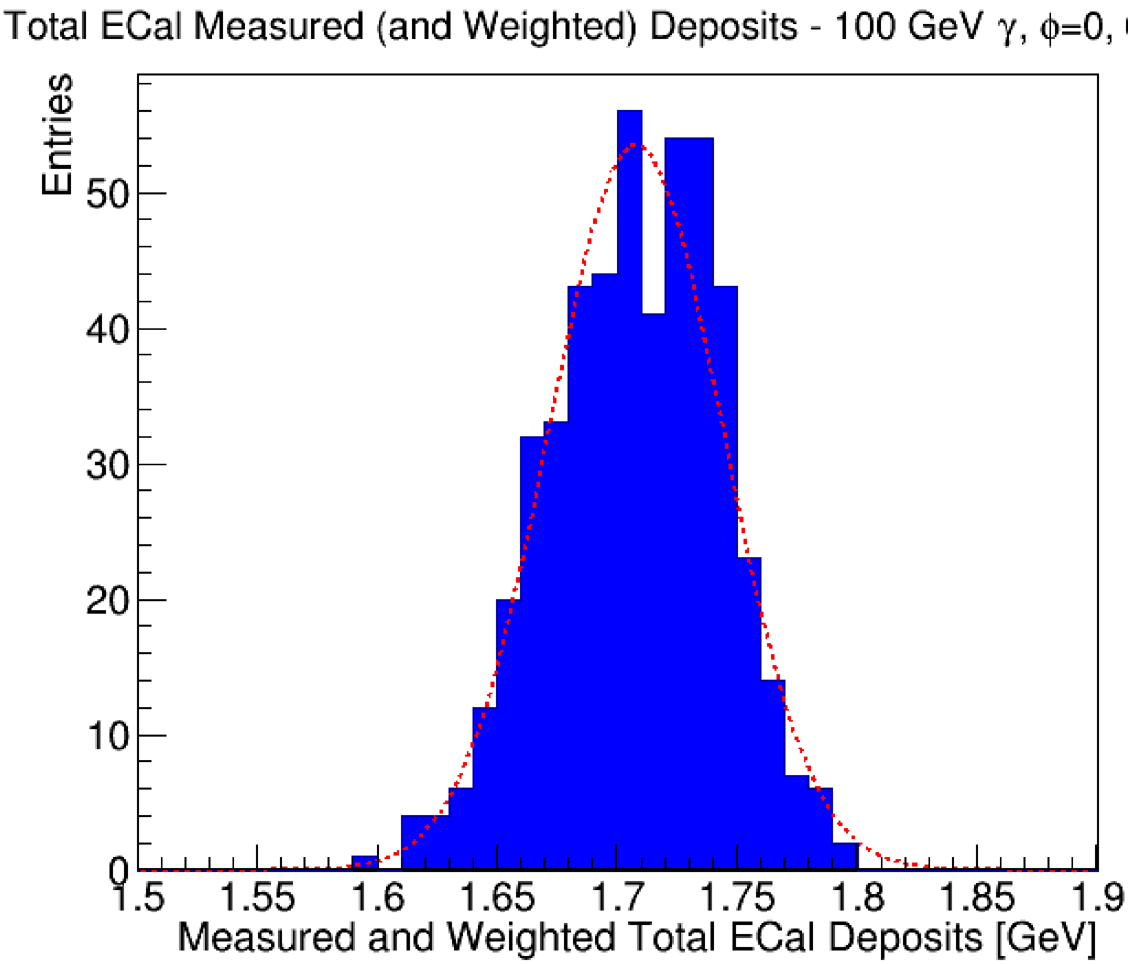

FIG. 5: Total measured (uncalibrated) charge deposits in the ECal, with deposits following thicker 5 mm absorber layers weighted by two to correct for the sampling fraction. This plot shows the recorded charge of 500 photons with an initial energy of 100 GeV at an angle of $\varphi = 0$. A Gaussian function (shown in dotted red) is fit to this distribution, and the Gaussian's mean and standard deviation are extracted. Here, the standard deviation is 2.1% of the mean. This fitting procedure is done for each φ angle under investigation.

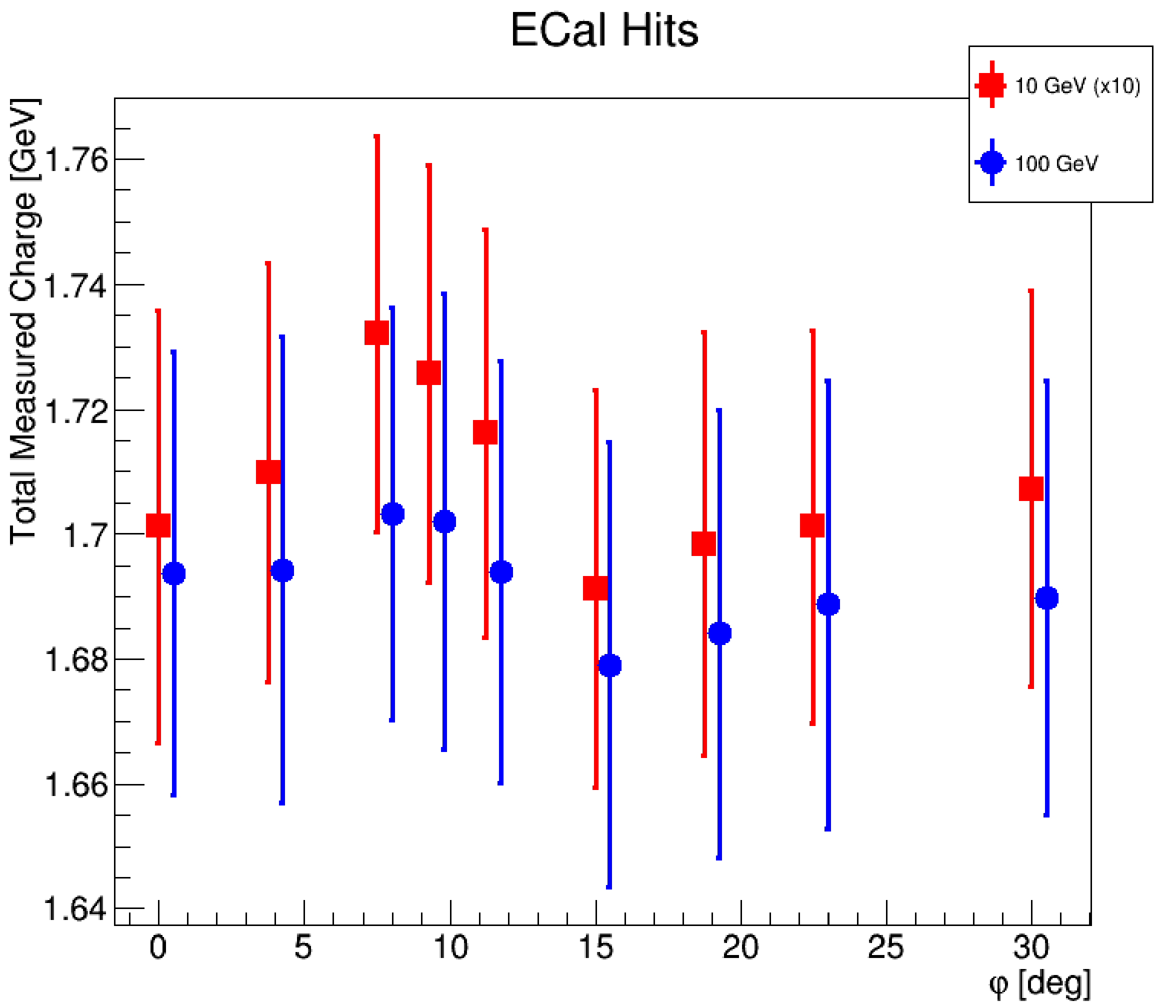

FIG. 6: The average weighted measured charge of 500 photon events of initial energies of 100 GeV (blue circles) and 10 GeV (red squares, scaled by ten) as a function of φ. The 100 GeV data set is artificially offset in φ for ease of comparison. Error bars indicate the standard deviation, which is constant across the full range (100 GeV and 10 GeV standard deviations are in the range of $2.0\% - 2.3\%$ and $5.7\% - 6.6\%$ of the mean, respectively). Both the 100 GeV and 10 GeV photon showers deposit slightly more charge ($\sim$0.5%) within the overlap region, likely due to the more frequent sampling (Fig. 4). The scaled 10 GeV runs deposit more charge in the calorimeter than the 100 GeV counterparts due more complete containment of the shower within the ECal. Deposits made beyond the ECal into the HCal are known as "leakage", and typically account for about 1% of measured shower energy for 100 GeV photons. The amount of leakage is greater for showers resulting from higher energy incident particles.

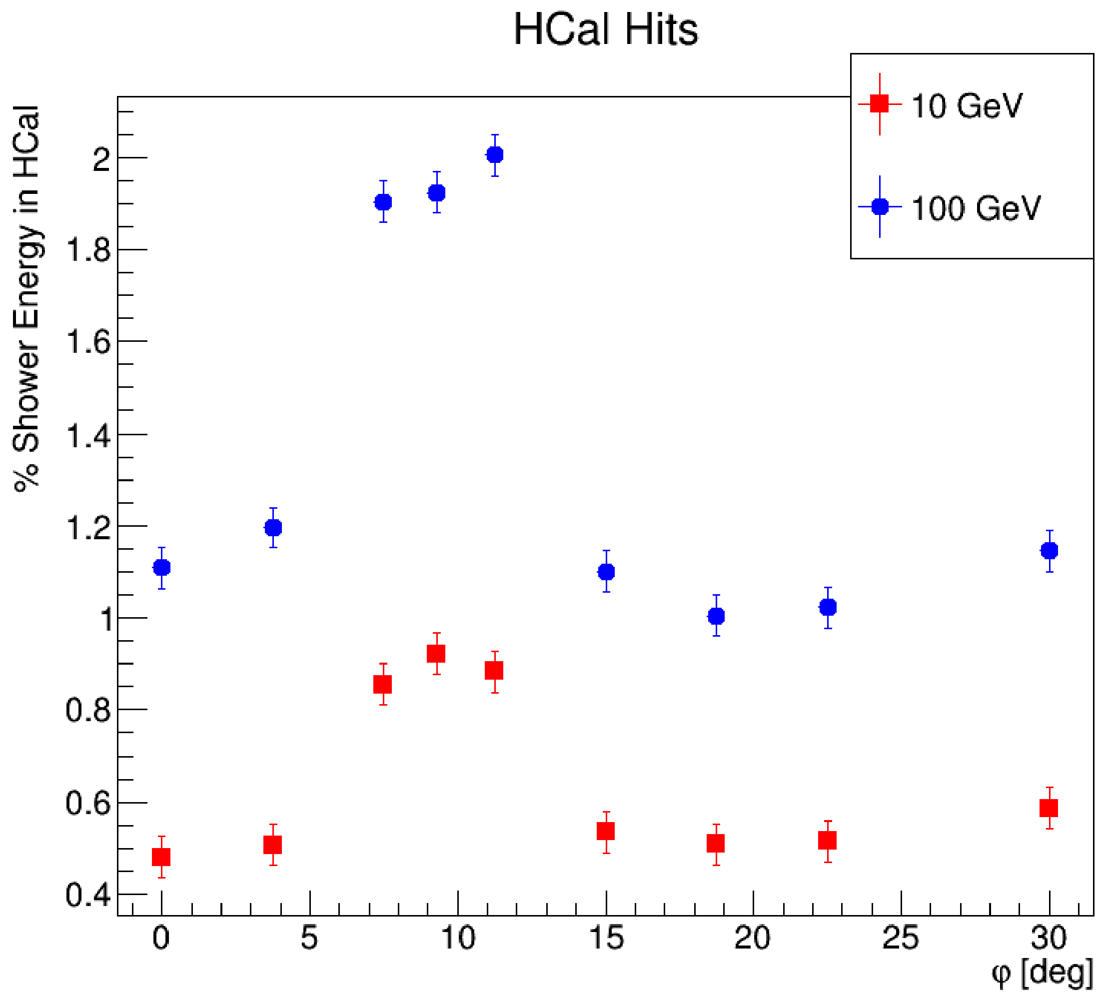

FIG. 7: The fraction of total measured shower energy in the HCal with 500 photon events of 100 GeV (blue circles) and 10 GeV (red squares, scaled by ten) initial energies as a function of φ. No weighting corrections are required for the HCal. The higher energy 100 GeV photons experience more leakage into the HCal than the less energetic 10 GeV runs. Deposits in the HCal notably see an increase in measured charge of more than 60% in the overlap region of the ECal. This is due to the thinner ECal depth within the this region (Fig. 3), where the number of radiation lengths decreases from 26 X_0 at normal incidence to a minimum of 23.7 X_0 at $\varphi = 8.786^o$.